

# Semi-Blind Maximum *a Posteriori* Fast Fading Channel Estimation for Multicarrier Systems

Mohamed SIALA, Emmanuel JAFFROT

CNET, 38-40 rue du Général Leclerc 92794 Issy les Moulineaux Cedex 9 France

mohamed.siala@cnet.francetelecom.fr, emmanuel.jaffrot@cnet.francetelecom.fr

**Résumé** – Dans cet article, un algorithme optimal d'estimation semi-aveugle de canal à évanouissements pour systèmes multiporteuses est proposé. Cet algorithme réalise une estimation itérative du canal multiplicatif au moyen du critère du maximum *a posteriori*, en utilisant l'algorithme 'Expectation-Maximization'. Cet algorithme nécessite une représentation appropriée du canal multiplicatif bi-dimensionnel temps-fréquence vu par les symboles multiporteuses transmis. Cette représentation est garantie par le théorème de décomposition orthogonale de Karhunen-Loève basé sur la fonction de corrélation temps-fréquence du canal.

**Abstract** – We propose in this paper an optimum semi-blind fast fading channel estimation algorithm for multicarrier systems. This algorithm performs an iterative estimation of the multiplicative channel according to the maximum *a posteriori* criterion, using the Expectation-Maximization algorithm. It requires a convenient representation of the two-dimensional frequency-time discrete multiplicative channel seen by all multicarrier transmitted symbols. This representation is guaranteed by the Karhunen-Loève expansion theorem based on the spaced-frequency spaced-time correlation function of the channel.

## 1 Introduction

We propose in this paper an optimum block-by-block two-dimensional semi-blind channel estimation algorithm for multicarrier systems. This algorithm performs an iterative channel estimation according to the maximum *a posteriori* (MAP) criterion, using the Expectation-Maximization (EM) algorithm [1, 2]. It uses profitably both pilot (or reference) symbols and information-carrying symbols in the optimization of channel estimation. It can also take into account the coded structure of the transmitted information-carrying symbols for an additional improvement of its performance. It requires a convenient representation of the multiplicative frequency and time selective fading channel using a Karhunen-Loève (KL) expansion [3] of the time-variant transfer function of the channel. This expansion relies on the spaced-frequency spaced-time correlation function of the two-dimensional fading channel [3]. The evaluation of the performance of this algorithm is based on a multicarrier system with reception diversity.

## 2 Transmitted signal characteristics

We consider a block-by-block two-dimensional channel estimation for multicarrier systems using PSK-modulated symbols. Each block is composed of  $N$  symbols  $a_{mn}$  with energy  $E_{mn}$  and two-dimensional frequency-time position  $(mF, nT)$ , where  $F$  and  $T$  are respectively the frequency and time spacing between two adjacent symbols. These symbols take their values from an arbitrary PSK alphabet set  $\Omega$  and are composed of  $N_D$  data symbols with (two-dimensional) indices in the set  $S_D$  and  $N_P$  pilot symbols with indices in the set  $S_P$ .

## 3 Multiplicative two-dimensional fading channel characteristics

We consider a multicarrier system with  $L$  decorrelated diversity branches. The time-variant transfer function [3] of the frequency and time selective fading channel seen at a given branch is characterized by its spaced-frequency spaced-time correlation function (SFSTCF)  $\phi(\Delta f, \Delta t)$ . For a channel scattering function [3] with classic Doppler power spectrum and exponential multipath intensity profile, the SFSTCF, with average power  $\phi(0, 0)$ , is given by

$$\phi(\Delta f, \Delta t) = \phi(0, 0) \frac{J_0(\pi B_d \Delta t)}{1 + j2\pi T_m \Delta f},$$

where  $B_d$  and  $T_m$  are respectively the Doppler and multipath spreads of the channel and  $J_0(\cdot)$  is the 0<sup>th</sup>-order Bessel function of the first kind.

## 4 Signal model at the output of the receiver matched filter

As depicted in figure 1, the multicarrier receiver is composed of  $L$  diversity branches provided by spatially decorrelated receiving antennas. We assume that the  $l^{\text{th}}$  diversity branch output signal associated to the symbol  $a_{mn}$  can be written as

$$R_{mn}^l = c_{mn}^l a_{mn} + N_{mn}^l,$$

where  $c_{mn}^l$  is the discrete channel gain factor of the  $l^{\text{th}}$  branch seen by the symbol  $a_{mn}$  and  $N_{mn}^l$  is a complex AWGN with variance  $N_0$ . The gain factors are independent from one diversity branch to the other but frequency and time correlated within the same branch.

Let  $(\cdot)^T$  denote the transpose operator. For notational convenience, we introduce the one-to-one indexing function  $\delta(k) = (m(k), n(k))$  between the one-dimensional

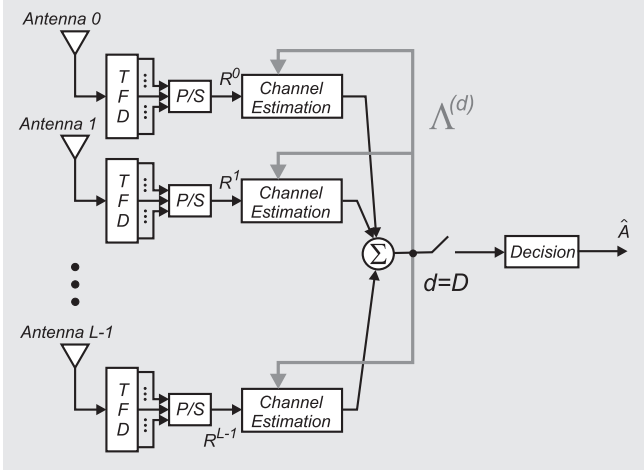


FIG. 1: Block diagram of the proposed receiver.

indexing set  $\{k\}_{k=0}^{N-1}$  and the two-dimensional indexing set  $S_D \cup S_P$ . We also introduce for each transmitted block the vector

$$\mathbf{R}^l = \left( R_{\delta(0)}^l, R_{\delta(1)}^l, \dots, R_{\delta(N-1)}^l \right)^T$$

of  $l^{th}$  branch matched filter outputs. Let also  $|\cdot|$  denote the absolute value operator. To get rid of the amplitude dependence of each PSK modulated symbol  $a_{mn}$  on its index  $(m, n)$ , we introduce the normalised block transmitted vector

$$\mathbf{A} = \left( A_{\delta(0)}, A_{\delta(1)}, \dots, A_{\delta(N-1)} \right)^T,$$

with  $A_{\delta(k)} = a_{\delta(k)} / |a_{\delta(k)}|$ . Based on this, we can rewrite the components of the  $l^{th}$  branch received vector  $\mathbf{R}^l$  as

$$R_{\delta(k)}^l = C_{\delta(k)}^l A_{\delta(k)} + N_{\delta(k)}^l,$$

where  $C_{\delta(k)}^l$  is the  $\delta(k)^{th}$  component of the equivalent discrete multiplicative fading channel vector

$$\mathbf{C}^l = \left( |a_{\delta(0)}| c_{\delta(0)}^l, |a_{\delta(1)}| c_{\delta(1)}^l, \dots, |a_{\delta(N-1)}| c_{\delta(N-1)}^l \right)$$

of the  $l^{th}$  branch.

## 5 Convenient representation of the discrete multiplicative fading channel

For MAP channel estimation, we need a convenient representation of the equivalent discrete fading channel seen at each diversity branch. This representation is based on a discrete version of the KL orthogonal expansion theorem [3].

**Proposition** The  $l^{th}$  diversity branch equivalent discrete fading channel vector  $\mathbf{C}^l$  can be expressed as

$$\mathbf{C}^l = \sum_{k=0}^{N-1} G_k^l \mathbf{B}_k,$$

where  $\{\mathbf{B}_k\}_{k=0}^{N-1}$  are the orthonormal eigenvectors of the equivalent discrete channel covariance matrix

$\mathbf{F} = E[\mathbf{C}^l \mathbf{C}^{l*T}]$  and  $\{G_k^l\}_{k=0}^{N-1}$  are independent complex zero-mean Gaussian random variables with variances equal to the eigenvalues  $\{\Gamma_k\}_{k=0}^{N-1}$  of the Hermitian matrix  $\mathbf{F}$ . The  $(p, q)^{th}$  entry of this matrix is given by

$$F_{pq} = \phi((m(p) - m(q)) F, (n(p) - n(q)) T) \sqrt{E_{\delta(p)} E_{\delta(q)}}.$$

The vectors  $\{\mathbf{G}^l\}_{l=0}^{L-1}$ , where  $\mathbf{G}^l = (G_0^l, G_1^l, \dots, G_{N-1}^l)^T$ , are referred to as the convenient representation of the equivalent discrete multiplicative channel seen at the output of the  $L$  diversity branches.

## 6 Maximum a posteriori discrete channel estimation

The MAP estimate  $\{\hat{\mathbf{G}}^l\}_{l=0}^{L-1}$  is given by

$$\{\hat{\mathbf{G}}^l\}_{l=0}^{L-1} = \arg \max_{\{\mathbf{G}^l\}_{l=0}^{L-1}} p(\{\mathbf{G}^l\}_{l=0}^{L-1} | \{\mathbf{R}^l\}_{l=0}^{L-1}).$$

Directly solving this equation is an intractable problem. However, the solution can be reached iteratively and easily by means of the EM algorithm. Given the  $L$  received vectors  $\{\mathbf{R}^l\}_{l=0}^{L-1}$ , the EM algorithm starts with an initial guess  $\{\mathbf{G}^{l(0)}\}_{l=0}^{L-1}$  of  $\{\mathbf{G}^l\}_{l=0}^{L-1}$ . As shown in figure 1, the evolution from the estimate  $\{\mathbf{G}^{l(d)}\}_{l=0}^{L-1}$  to the new estimate  $\{\mathbf{G}^{l(d+1)}\}_{l=0}^{L-1}$  is performed  $D$  times via the auxiliary function of the EM algorithm.

**Proposition** The  $p^{th}$  component of the  $l^{th}$  branch reestimate  $\mathbf{G}^{l(d+1)}$  is explicitly given by

$$G_p^{l(d+1)} = w_p \sum_{k=0}^{N-1} R_{\delta(k)}^l \times \left( \sum_{A \in \Omega} AP \left( A_{\delta(k)} = A \{\mathbf{R}^l\}_{l=0}^{L-1}, \{\mathbf{G}^{l(d)}\}_{l=0}^{L-1} \right) \right)^* B_{p\delta(k)}^*,$$

where  $B_{p\delta(k)}$  is the  $k^{th}$  component of  $\mathbf{B}_p$  and

$$w_p = \frac{1}{1 + N_0/\Gamma_p}.$$

When the normalized transmitted vector  $\mathbf{A}$  is coded, the conditional probabilities of  $A_{\delta(k)}$  can be computed by means of the Bahl algorithm [4].

For uncoded information-carrying symbols with centrosymmetric PSK modulation, we can use

$$G_p^{l(0)} = w_p \sum_{\delta(k) \in S_P} R_{\delta(k)}^l D_{\delta(k)}^* B_{p\delta(k)}^*$$

as  $p^{th}$  component of the initial guess  $\mathbf{G}^{l(0)}$ , where  $D_{\delta(k)}$  is the value taken by the pilot symbol  $A_{\delta(k)}$ ,  $\delta(k) \in S_P$ .

Let  $\mathcal{R}(\cdot)$  denote the real part operator. For uncoded BPSK modulated symbols, the previous expression of

$G_p^{l(d+1)}$  can be simplified into

$$G_p^{l(d+1)} = w_p \left( \sum_{\delta(k) \in S_D} R_{\delta(k)}^l \tanh \left[ 2\mathcal{R}e \left\{ \Lambda_{\delta(k)}^{(d)} \right\} \right] B_{p\delta(k)}^* + \sum_{\delta(k) \in S_P} R_{\delta(k)}^l D_{\delta(k)}^* B_{p\delta(k)}^* \right),$$

where

$$\Lambda_{\delta(k)}^{(d)} = \frac{1}{N_0} \sum_{l=0}^{L-1} R_{\delta(k)}^l \left( \sum_{p=0}^{N-1} G_p^{l(d)*} B_{p\delta(k)}^* \right).$$

## 7 Simulation results

We present below some simulation results for a 16-carrier OFDM system with BPSK modulated symbols. We restrict our investigation to time-frequency blocks with 256 data and pilot symbols and either 16 or 4 pilot symbols per block for channel estimation. The positions of these pilot symbols within each time-frequency block are specified in Figure 2.

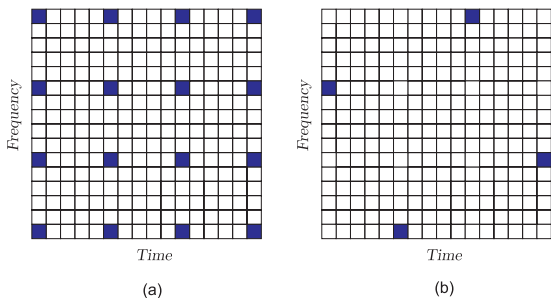


FIG. 2: Pilot symbols positions within a time-frequency block for 16 (a) and 4 (b) pilot symbols.

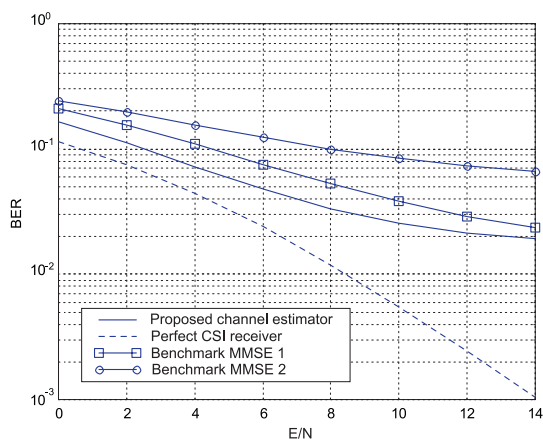


FIG. 3: Bit Error Rate for 16 pilots,  $B_d T_m = 10^{-3}$  and  $L = 2$ .

For illustration, we assume that all data and pilot symbols have a common energy  $E$ . Moreover, we evaluate the performance of our algorithm for three severe channels with  $B_d T_m = 10^{-3}$ ,  $10^{-4}$  and  $10^{-6}$ , and  $L = 2$  and 4 diversity branches.

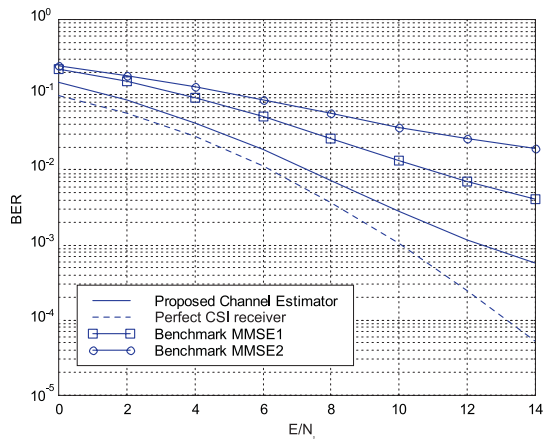


FIG. 4: Bit Error Rate for 16 pilots,  $B_d T_m = 10^{-3}$  and  $L = 4$ .

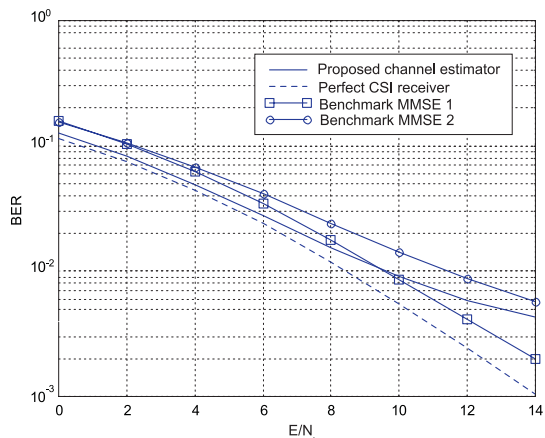


FIG. 5: Bit Error Rate for 16 pilots,  $B_d T_m = 10^{-4}$  and  $L = 2$ .

For the sake of simplicity, we restrict the number of iterations  $D$  carried by our algorithm to 5. This number is deemed to be sufficient for almost reach the best asymptotic achievable raw BER.

The performance of our algorithm is compared to two benchmarks based on the MMSE criterion. The first benchmark, referred to as MMSE 1, carries out a linear channel estimation based on a plane surface interpolation of the channel seen at the pilot symbols positions. The second benchmark, referred to as MMSE 2, carries out channel estimation by interpolating the channel seen at the pilot symbols positions with a constant plane surface.

The performance of our algorithm is also compared to the simulated and theoretical performance of the hypothetical receiver with perfect channel state information (CSI). We recall that the theoretical performance of this receiver is given by the bit error probability [3]

$$P_e = \left( \frac{1-\mu}{2} \right)^L \sum_{l=0}^{L-1} \binom{L-1+l}{l} \left( \frac{1+\mu}{2} \right)^l$$

of the uncoded BPSK over a Rayleigh multipath fading channel with  $L$  branches of diversity, with

$$\mu = \sqrt{\frac{E/N_0 L}{1 + E/N_0 L}}.$$

As shown in Figures 3 through 8, for the critical chan-

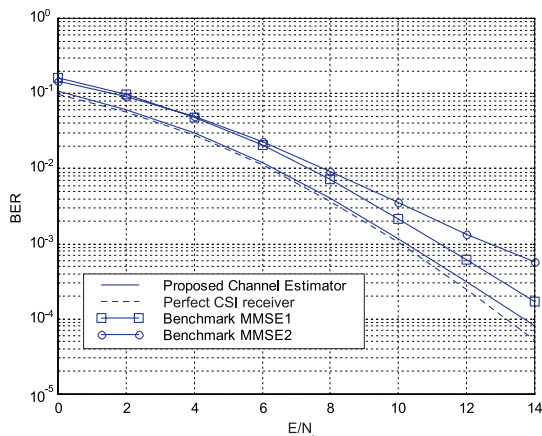


FIG. 6: Bit Error Rate for 16 pilots,  $B_d T_m = 10^{-4}$  and  $L = 4$ .

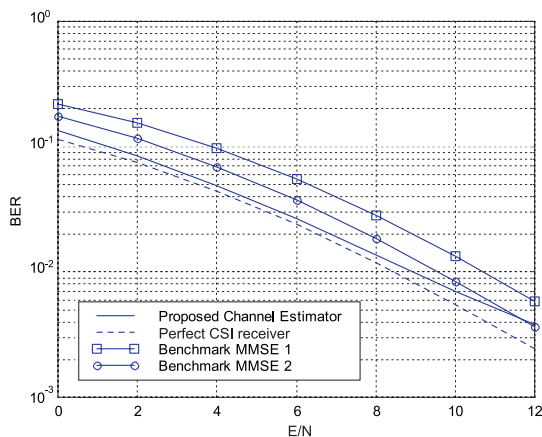


FIG. 7: Bit Error Rate for 4 pilots,  $B_d T_m = 10^{-6}$  and  $L = 2$ .

nels or the reduced number,  $N_P = 4$ , of pilot symbols we have considered above, the considered benchmarks present a significant degradation with respect to our algorithm. This degradation is notable especially for high values of the BER and the number of diversity branches  $L$  and low values of the number of pilot symbols  $N_P$ . Moreover, as illustrated in Figures 4, 6 and 8, our algorithm provides a good robustness against channel estimation imperfections for a large number of diversity branches and a low number of pilot symbols.

By way of example, for a severe channel with  $B_d T_m = 10^{-3}$  and a raw BER of  $10^{-3}$ , Figure 4 shows that the gain provided by our algorithm is around 3.5 dB with respect to the most favorable of the considered MMSE-based benchmarks. Moreover, for the same raw BER, this figure shows that our algorithm presents a degradation of only 1 dB with respect to the perfect CSI receiver.

As illustrated in Figure 6, even for less severe channels with  $B_d T_m = 10^{-4}$ , where both considered benchmarks show a good performance, our algorithm still guarantees a gain of 1 dB at a raw BER of  $10^{-3}$  with respect to the most favorable of the MMSE-based algorithm and presents a degradation of less than 0.2 dB with respect to the perfect CSI receiver.

As shown in all figures, the BER curves corresponding to our algorithm present some kind of flattening at high

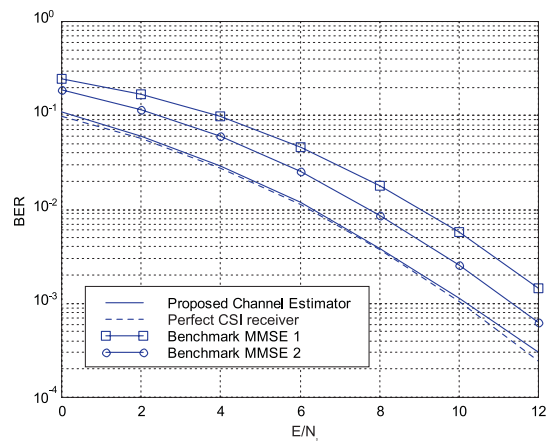


FIG. 8: Bit Error Rate for 4 pilots,  $B_d T_m = 10^{-6}$  and  $L = 4$ .

values of  $E/N_0$  for reduced numbers of diversity branches,  $L$ , and pilot symbols,  $N_P$ , and large values of  $B_d T_m$ . This flattening is due to the sensitivity of our gradient-like iterative algorithm to the way its initial conditions are computed. This problem can be solved by using one of the two presented benchmarks for the initialization of the proposed algorithm.

## 8 Conclusion

We have proposed an iterative receiver with spatial diversity using a semi-blind maximum *a posteriori* estimation of the multipath fading channel. Based on simulation results, we have noticed that the degradation in performance presented by this algorithm with respect to perfect channel state information is very small compared to more intuitive algorithms.

## References

- [1] A. P. DEMPSTER, N. M. LAIRD, and D. B. RUBIN, *Maximum Likelihood from Incomplete Data via the EM algorithm*, Journal of the Royal Statistical Society, Ser. 39, 1977.
- [2] G. K. KALEH, *Joint Carrier Phase Estimation and Symbol Decoding of Trellis Codes*, European Transactions on Telecommunications and Related Technology, no. 2, March-April 1993.
- [3] J. G. PROAKIS, *Digital Communications*, McGraw Hill, New York, 1989.
- [4] L. R. BAHL, J. COCKE, F. JELINEK and J. RAVIV, *Optimal Decoding of Linear Codes for Minimizing Symbol Error Rate*, IEEE Transactions on Information Theory, vol. IT-20, March 1974.
- [5] M. SIALA and D. DUPONTEIL, *Maximum A Posteriori Multipath Fading Channel Estimation for UTRA/FDD*, FRAMES Workshop '99, Delft, The Netherlands, January 1999.